Parameters of Radiation-Induced Centers for Simulation of Irradiated Power Devices

Ralf Siemieniec, Josef Lutz, Winfried Südkamp, Reinhard Herzer

Abstract— **Irradiation techniques are widely used for carrier lifetime control especially in power devices because of their good reproducibility. Simulation lacks of missing or incomplete recombination center data despite the fact of suitable recombination models. In these work we used center data estimated by DLTS and lifetime measurements for the simulation of electron radiated devices and compare the results with the measured device characteristics.**

I. Introduction

Lifetime control by use of irradiation techniques is widely used for the optimization of power device characteristics. Radiation induced centers are about to replace the conventional impurities gold and platinum because of the possibility of more exact process control. While electron irradiation results in a homogenous lifetime profile the use of proton- or alpha-particles leads to local lifetime profiles. The combination of different irradiation types offers the possibility to generate almost any wished lifetime profile which is advantageous in comparison to the use of gold or platinum [7].

It is fairly known, that the use of an extended recombination model allows improved device simulations explaining stationary and dynamical device characteristics [9], [12]. Furthermore such models allow to consider effects caused by trap charging processes as in case of IMPATT oscillations [8]. Thus, the main problem is the knowledge of the recombination center properties.

II. Samples

For examination purposes freewheeling diode samples were prepared using neutron transmutation doped float zone silicon wafers. The devices with a pin-structure have a wide nn^+-junction and a pn-junction depth of app. 20μm. The blocking voltage of all samples is 1200V, therefore the base width is about 90μm. With an active area of 6mm^2 the rated current is 10A or 166A/cm^2. The different electron irradiation types applied to these samples are shown in Table I. After irradiation, all devices were annealed at a temperature higher than 300°C for one hour.

III. Recombination Model

Irradiation processes generate a number of recombination centers with different energy levels in the band gap of Silicon. Each of these levels may act as a recombination center. The total recombination rate results from the capture and emission processes of each level. Therefore, an extended recombination model is necessary which considers the full trap dynamics of a number of independent recombination centers.

Ralf Siemieniec is with the Department of Solid-State Electronics at the Technische Universitaet Ilmenau, Germany, E-mail:ralf.siemieniec@tu-ilmenau.de; Winfried Südkamp is with the Aktiv-Sensor GmbH, Stahnsdorf, Germany; Josef Lutz is with the Faculty of Electrical Engineering and Information Technology at the Technische Universitaet Chemnitz, Germany; Reinhard Herzer is with the Semikron Elektronik GmbH Nürnberg, Germany

TABLE I
Sample overview

Sample	Type	Energy [MeV]	Dose [cm^{-2}]
N	n-Si	-	-
11E1	n-Si	1.1	$1 \cdot 10^{14}$
11E2	n-Si	1.1	$5 \cdot 10^{14}$
11E3	n-Si	1.1	$1 \cdot 10^{15}$
100E1	n-Si	10	$3.2 \cdot 10^{13}$
100E2	n-Si	10	$6.4 \cdot 10^{13}$
100E3	n-Si	10	$1.1 \cdot 10^{14}$

For all simulations, we used the 2D device simulator TeSCA [2]. This tool solves the Poisson equation and the electron and hole current continuity equations which have been extended for the consideration of deep traps as described in [9].

IV. Parameter Determination

The fundamental properties of the irradiation-induced recombination centers are determined by means of DLTS measurements [5]. In case of E(90K), the hole capture rate has been measured in electron-irradiated p-type Silicon [11]. The trap E(230K) is not found in the samples 11E1-11E3 most probably due to the annealing process.

E(90K) controls the high-level lifetime τ_{HL} which is most important since bipolar power devices are operated at high-injection during on-state and turn-on/turn-off. Thus it is necessa-

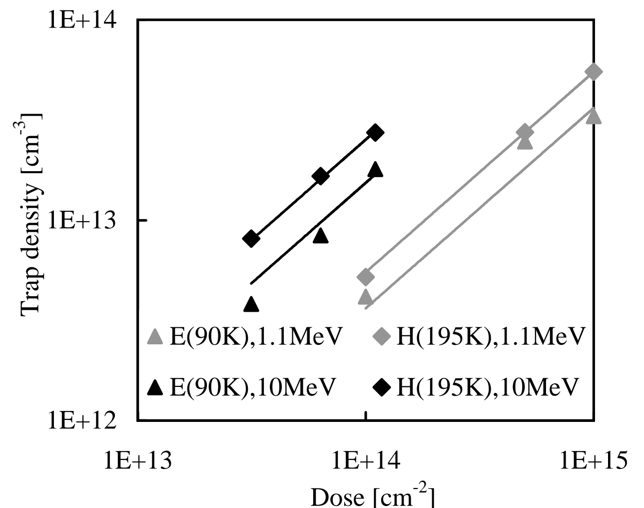

Fig. 1
Trap concentration vs. irradiation dose

TABLE II
CAPTURE RATES

	Electron Capture Rate c_n [cm^3s^{-1}]	Hole Capture Rate c_p [cm^3s^{-1}]
E(90K)	$1.15\cdot10^{-7}\exp\left(-\frac{T}{355.4K}\right)$	$6.39\cdot10^{-7}\sqrt{\frac{T}{300K}}\exp\left(\frac{6.15\cdot10^{-3}\,eV\,K}{k_BT}\right)$
E(230K)	$3.41\cdot10^{-8}\sqrt{\frac{T}{300K}}\exp\left(\frac{22.13\cdot10^{-3}\,eV\,K}{k_BT}\right)$	$2.79\cdot10^{-8}\sqrt{\frac{T}{300K}}\exp\left(-\frac{22.13\cdot10^{-3}\,eV\,K}{k_BT}\right)$
H(195K)	$3.41\cdot10^{-8}\sqrt{\frac{T}{300K}}\exp\left(\frac{85\cdot10^{-3}eV\,K}{k_BT}\right)$	$4.3\cdot10^{-9}\sqrt{\frac{T}{300K}}$

ry to estimate the capture rates of E(90K) in a wide temperature range. The data of E(90K) found by DLTS are measured at temperatures of 80...100K which is far outside of the operating temperature of power devices of 300...400K. An extrapolation of the DLTS data is not possible due to the wide temperature range [1]. While the electron capture rate is reasonable small compared to the hole capture rate of E(90K), measurements of the high-level lifetime were used for the estimation of the electron capture rate. Figure 1 shows the center concentration in dependence of irradiation dose. Due to the approximately linear dependency of concentration on dose and by considering the lifetime τ_0 of the non-irradiated Silicon equation 1 is used for the determination of the electron capture rate of E(90K):

$$\frac{1}{\tau_{HL}} = c_N N_T + \frac{1}{\tau_0} \qquad (1)$$

The plot of the inverse high-level lifetime τ_{HL} versus trap concentration N_T allows the estimation of the electron capture rate of E(90K). Since E(90K) is a comparatively shallow trap, a high excess carrier concentration is necessary to meet the preconditions for the validity of the high-injection approximation. Therefore we used OCVD (Open Circuit Voltage Decay) measurements [6] with optical excitation of excess carriers by means of Laser light pulses [10]. To achieve a homogenous excess carrier concentration vertically along the low-doped base region a YAG laser with the primary wavelength of 1064nm is used due to the low absorption coefficient of $10cm^{-1}$ [3], [4]. The maximum generated excess concentration is about $2\cdot10^{17}cm^{-3}$.

Table II shows the results for the capture rates of the relevant recombination centers.

V. Simulation results

As examples we first compared the forward characteristics of a number of different samples as shown in figures 2 and 3. Since series resistances (bonding wires etc.) influences forward characteristics significantly, these resistances were measured in dependency on temperature and eliminated in the measurement results. The agreement between measurements and simulations found here is good, especially if one considers that a current of 30A corresponds to a current density of $500A/cm^2$ or the triple nominal current.

Further the forward voltage dependency on temperature at rated current for different samples is investigated. The comparison is shown in figures 4 and 5. Under these conditions we found a good agreement between measurement and simulation. The dependence of forward voltage on temperature is from further interest since it is very important for paralleling of devices as usually done in modules, therefore an appropriate simulation tool could support development of radiated power devices. Generally it is preferable to achieve a positive temperature coefficient which means a higher forward voltage at higher temperature for a con-

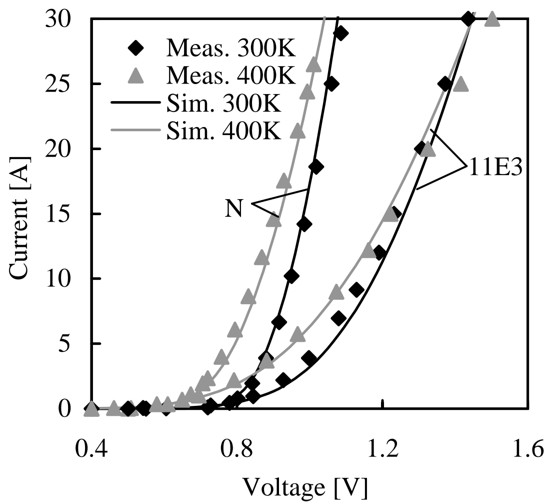

Fig. 2
FORWARD CHARACTERISTICS OF SAMPLES N AND 11E3

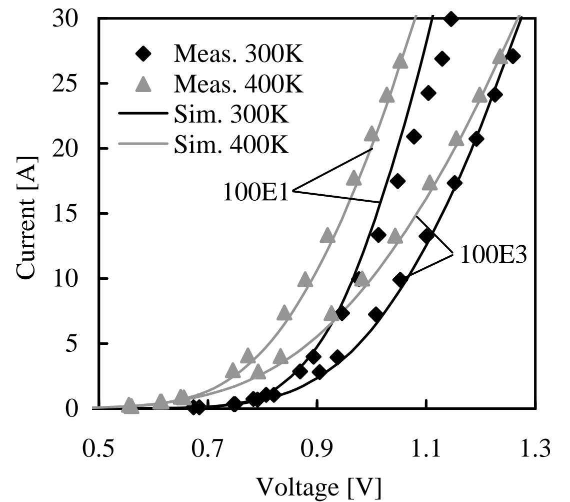

Fig. 3
FORWARD CHARACTERISTICS OF SAMPLES 100E1 AND 100E3

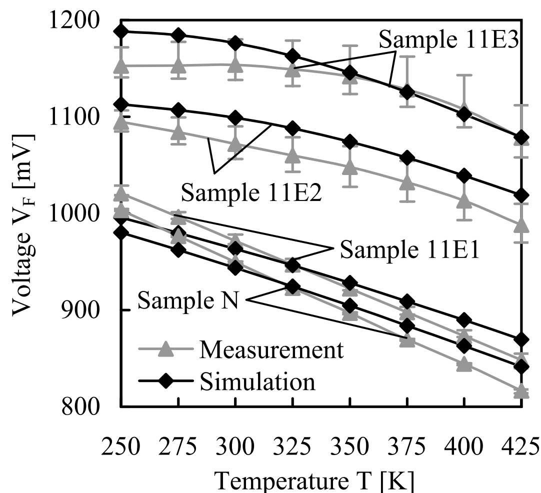

Fig. 4

TEMPERATURE DEPENDENCE OF FORWARD VOLTAGE OF SAMPLES N, 11E1 AND 11E3 ($J = 166A/cm^2$)

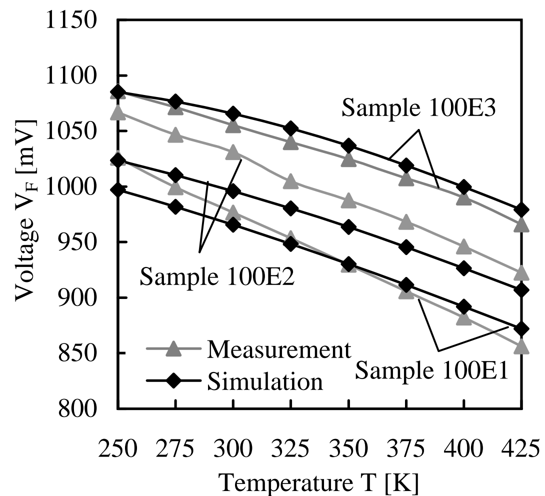

Fig. 5

TEMPERATURE DEPENDENCE OF FORWARD VOLTAGE OF SAMPLES 100E1-100E3 ($J = 166A/cm^2$)

stant current.

Reverse recovery measurements were done using a common step-down converter circuit against an inductive load. For appropriate device simulation, TeSCA allows to include different discrete structures (as IGBT and freewheeling diode) and to connect them by boundary conditions - a kind of mixed-mode simulation.

By switching the diode from forward conducting state to the blocking state, the stored charge (the excess carriers) is removed by recombination processes and by the reverse recovery current. In the moment when the carrier density at the pn-junction is in the order of the thermal equilibrium concentration a space-charge region is formed and the reverse current declines. The voltage across the diode is controled by the external circuit, in case of reasonable large inductances the current slope after the reverse recovery current peak generates large spikes in the reverse voltage. The recovery behavior itself is governed by the dynamics of the stored charge. The analysis of the carrier distribution inside bipolar power devices explains the device properties and supports the optimization of devices.

The value of the stored charge in a given device depends mainly on forward current and temperature. Figures 6 and 7 compare the stored charge of different samples at temperatures of 300K and 400K as a result of reverse recovery measurements and simulations. As before a good agreement of simulations and measurements is found. The comparison of the reverse recovery waveforms on example of sample 100E3 in figures 8 and 9 shows excellent agreement.

VI. CONCLUSION

The properties of the most important radiation-induced traps after annealing are determined and used in device simulation. For simulation purposes an extended recombination model is used for considering a number of different recombination centers as found as a result of carrier lifetime adjustment steps. This model further considers the charging processes of the generated traps and therefore allows a physically correct description of recombination processes under different injection conditions.

Difficulties concerning the validity of lifetime measurements as used for the parameter determination of the dominant recombination center E(90K) were overcome by the use of laser light pulses for generation of excess carriers.

The presented simulation results explain the static and dynamic behavior of the investigated samples as well as their temperature dependencies. Device simulation of radiated bipolar devices may therefore be used for development, optimization and understanding of radiated devices.

ACKNOWLEDGEMENTS

The authors wish to thank the scientists from the Weierstrass Institute for Applied Analysis ans Stochastics in Berlin, especially Dr. Nürnberg, Dr. Stefan and Prof. Gajewski, who developed the device simulator TeSCA and give great support by implementing new features and algorithms into the simulation

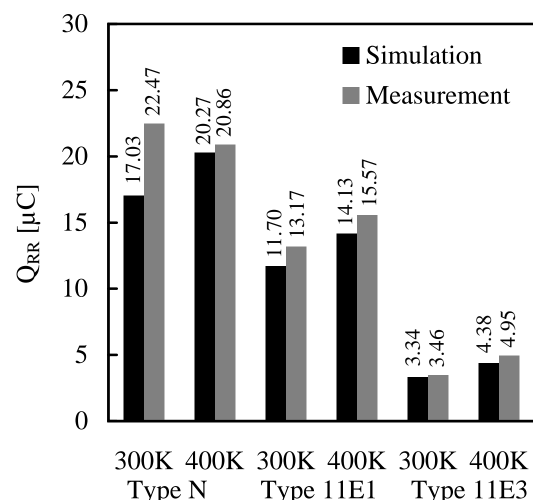

Fig. 6

Q_{RR} FOR SAMPLES N, 11E1 AND 11E3 ($V_R = 250V$, $I_F = 10A$)

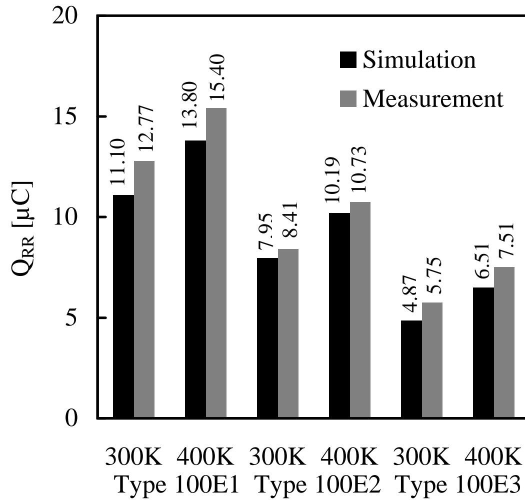

Fig. 7

Q_{RR} FOR SAMPLES 100E1-100E3 ($V_R = 250V$, $I_F = 10A$)

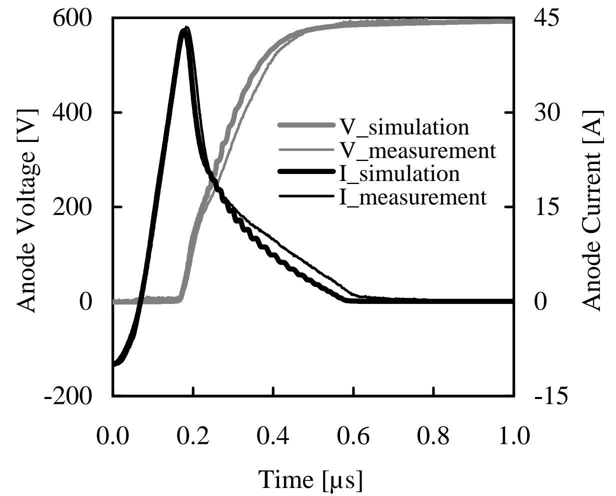

Fig. 9

REVERSE RECOVERY OF SAMPLE 100E3 (I_F=10A,V_R=600V, DI/DT=500A/μS, T=400K)

system.

This work is supported by grants of the Deutsche Forschungsgemeinschaft.

REFERENCES

[1] H. Bleichner, P. Jonsson, and N. Keskitalo. Temperature and injection dependence of the Shockley-Read-Hall-lifetime in electron irradiated n-type silicon. *Journal of Applied Physics*, 79(12):9142–9148, 1996.

[2] H. Gajewski, B. Heinemann, and H. Langmach. *TeSCA-Handbuch*. Weierstrass-Institut für Mathematik, 1991.

[3] S. Gall. *Admittanzspektroskopische Untersuchungen des a-SiH/c-Si-Heteroüberganges im Hinblick auf photovoltaische Anwendungen*. Dissertation TU Berlin, 1997.

[4] V. Grivickas. An accurate method for determining intrinsic optical absorption in indirect band gap semiconductors. *Solid-State Communications*, 108(8):561–566, 1998.

[5] D. V. Lang. Deep-level transient spectroscopy: A new method to characterize traps in semiconductors. *Journal of Applied Physics*, 45(7):3023–3032, 1974.

[6] S. R. Lederhandler and L. J. Giacoletto. Measurement of Minority Carrier Lifetime and Surface Effects in Junction Devices. In *Proc. IRE*, pages 477–483, 1955.

[7] J. Lutz and U. Scheuermann. Advantages of the new Controlled Axial Lifetime Diode. In *Proc. PCIM*, 1994.

[8] J. Lutz, W. Südkamp, and W. Gerlach. Impatt Oscillations in Fast Recovery Diodes due to Temporarily Charged Radiation-Induced Deep Levels. *Solid-State Electronics*, 42(6):931–938, 1998.

[9] R. Siemieniec, W. Südkamp, and J. Lutz. Simulation and Experimental Results of Irradiated Power Diodes. In *Proc. EPE*, 1999.

[10] R. Siemieniec, W. Südkamp, and J. Lutz. Determination of Parameters of Radiation Induced Traps in Silicon. *Solid-State Electronics*, 2002. to be published.

[11] W. Südkamp and W. Gerlach. *Untersuchung tiefer Zentren und Bauelementesimulation*. VDI/VDE-IT, 1999. Reihe Innovationen in der Mikrosystemtechnik.

[12] J. Vobecky, P. Hazdra, and J. Voves. Accurate Simulation of Combined Electron and Ion Irradiated Silicon Devices for Local Lifetime Tailoring. In *Proc. ISPSD*, pages 265–270, 1994.

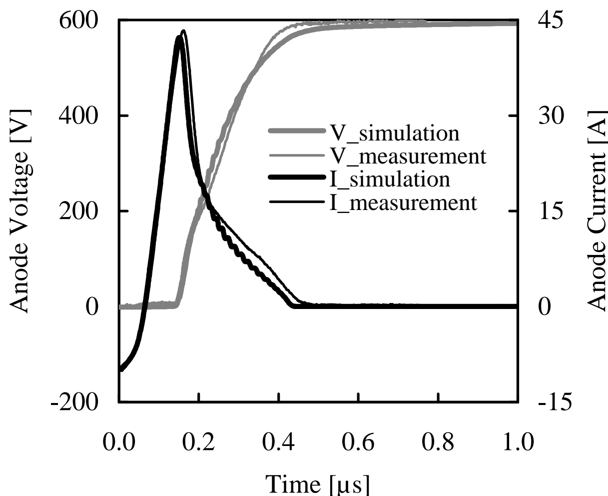

Fig. 8

REVERSE RECOVERY OF SAMPLE 100E3 (I_F=10A, V_R=600V, DI/DT=500A/μS, T=300K)